

ON THE RESPONSE OF THE SMALL BUILDINGS TO VIBRATIONS

L.Munteanu¹, V.Chiroiu², and T.Sireteanu²

¹ Institute of Solid Mechanics, Romanian Academy
Ctin Mille 15, Bucharest 010141
e-mail: ligia_munteanu@hotmail.com

² Institute Solid Mechanics, Romanian Academy
Ctin Mille 15, Bucharest 010141
e-mail: veturiachiroiu@yahoo.com; e-mail: siretimsar@yahoo.com

Keywords: Small building, Electromechanical device, Harmonic excitation, Time-dependent frequency, Random earthquakes.

Abstract. *In this work, the analysis the response to vibrations of a small building equipped with an electromechanical vibration absorber is investigated. In the first part, the case of harmonic excitation with constant or time dependent frequencies is considered, and in the second part, the case of random earthquakes, respectively. The cross correlation functions and the mean square displacements are calculated for the structure when it is equipped with an electromechanical vibration absorber. The stochastic process which characterizes the earth movements is coupled to the cnoidal method which delivers the analytical solutions of the nonlinear problem. The interaction between the structure and the energy source is analyzed via the Sommerfeld effect inside the resonance region. The resonance capture and the vibration reduction are displayed by the time history responses of the displacement and angular velocities above the resonance.*

1 INTRODUCTION

Deterministic evaluation of the response of the buildings subjected to earthquakes is a valuable tool in obtaining information on the behavior of structures under forces which are statistical in nature [1]-[3]. The influence of the time histories of external excitations on the dynamics of structures can be explored both theoretically and experimentally [4], [5].

The theoretical description involves the explicit treatment of both cases, i.e. the harmonic excitation with constant and time dependent frequency. The description asked the temporal characteristics of the seismic data and the response of buildings to transient and seismic excitations.

An attempt to apply the methods of stochastic processes in the analysis of tall buildings to random earthquakes was made by Eringen [6]. This method is based on the cross correlations functions from which the mean square displacements can be evaluated. This model was applied in the electrical circuits [7], in discrete element strings [8] and other problems. The earth movements in the boundary condition can be expressed under the form of expected values.

In this paper, the response of a building to vibrations is analyzed when an electromechanical vibration absorber is attached to the last story of the building.

In the first part of this article the case of harmonic excitation is considered, while the second part will consider the case of random earthquakes.

The reduction of vibrations for a resonant structure was studied by Felix, Balthazar and Brasil [9], [10] and Souza et al. [11] using tuned liquid column. A tuned liquid column connected to the structure works due to the inertial secondary system principle, by which the damper counteracts the forces producing the vibration.

Nagem, Madanshetty and Medhi [12] have experimentally analyzed the reduction of vibrations for a system consisted from a cantilever beam and a motor, by using a linear electromechanical vibration absorber and an ideal eccentrically motor with a sinusoidal force. Bolla et al, [13] have reported approximate analytical solutions to nonlinear vibrating problem, excited by a nonideal motor. A device of nonlinear electromechanical vibration absorber with a nonlinear function of type Rayleigh oscillator was introduced by Yamapi et al. [14].

The case of a nonideal eccentrically motor or a source of limited power supply was investigated by Felix and Balthazar [14] for a nonlinear friction of type cubic-quintic Duffing oscillator. This kind of devices with nonlinear resistor and capacitor were studied by Yamapi et al. [15], Yamapi and Wofo [16], [17] and Mbouna Ngueuteu, Yamapi and Wofo [18].

We are interested in this paper on the case when the vibrating system and the energy source interact with one another. This interaction corresponds to the non-ideal systems or the systems with non-ideal excitation and it is explained by the Sommerfeld effect which says that the steady state frequencies of the DC motor increase with respect to the power, and when the structure resonates with the source, a part of the source energy is used to generate large vibrations. These vibrations can counteract the vibrations of the forced structure, without changing the motor frequency. We must mention that the power is supplied in a step-by-step manner.

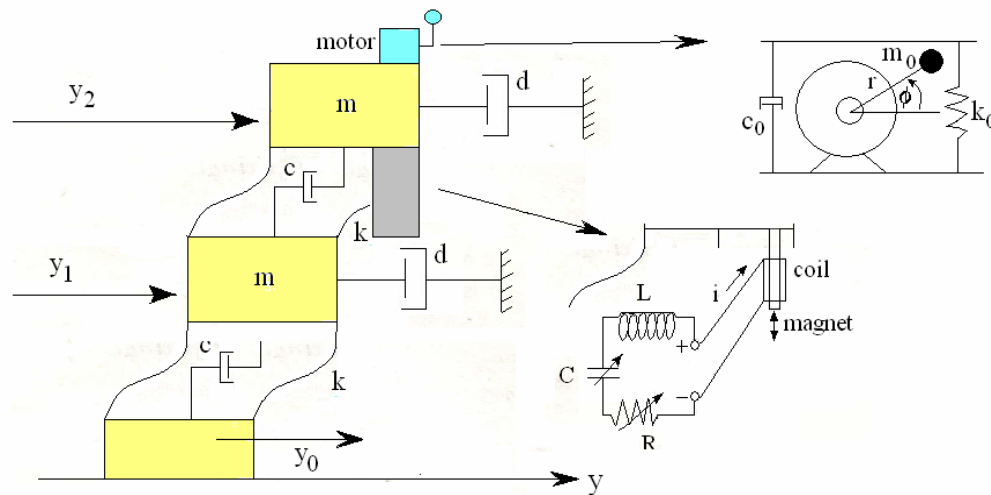


Figure 1. Scheme of the building coupled to a vibration absorber device.

For sufficient motor power, a jump can occur. i.e. the frequency increases and the vibrations decrease, resulting in lower power consumption by the motor [14], [19], [20]. The Sommerfeld effect results from the balance of the energy and it is due to the coupling between the excitation mechanism and the vibrational loads [21].

In this paper we consider a small building with two stories (See Fig. 1). The second floor is equipped with an electromechanical vibration absorber. The structure may be characterized by the stiffness and damping which can be considered to be either the cubic Duffing, cubic-quintic Duffing or Rayleigh, or another such as the Van der Pol with first, second, third, fourth and fifth term.

In the problem considered here, the stiffness is expressed as a sum of a linear and a cubic Duffing term, while the damping is considered to be linear.

Because of the stiffness nonlinearity, the equations cannot be solved by usually applied Fourier-integral type of solutions. The inverse scattering theory generally solves such nonlinear differential equations. Osborne [22] has suggesting that the method is reducible to a generalization of the Fourier series with the cnoidal functions as the fundamental basis function. This is because the cnoidal functions are much richer than the trigonometric or hyperbolic functions, that is, the modulus \tilde{m} of the cnoidal function, $0 \leq \tilde{m} \leq 1$, can be varied to obtain a sine or cosine function ($\tilde{m} \cong 0$), a Stokes function ($\tilde{m} \cong 0.5$) or a solitonic function, sech or tanh ($\tilde{m} \cong 1$) [23].

The paper is structured as follows: Section 2 presents the model equations for a small building with the electromechanical vibration absorber attached to the last story. The electromechanical device is consisted of a DC motor coupled magnetically by the building. The structure is subjected to external harmonic excitation and also to the excitation of the source with limited power supply. Section 3 presents the solutions written in the terms of the *theta function* representation as a sum of linear and nonlinear superposition of cnoidal vibrations. Some aspects of the dynamics of the building equipped with an electromechanical vibration absorber are discussed in Section 4 for the case of a constant excitation frequency, emphasizing the role of the additional equation which includes the transfer of the source energy to the structure. Next section explores the case of the time-dependent excitation frequency, focusing on the effectiveness of the vibration reduction. The time history responses of the displacement

and angular velocities above the resonance are presented for both cases in order to understand the interaction structure- energy source. Finally, the Section 6 treats the case of random earthquakes modeled as a stochastic or random process. The earthquakes are of short duration and therefore the stationary character of the process is questionable.

2 FORMULATION OF THE PROBLEM

The presence of the vibration absorber device is expressed mathematically by coupling between the motion equations of the building and the equations of the energy source. The resistive torque applied to the motor is neglected. The motion equations are given by

$$m\ddot{y}_1 + c(2\dot{y}_1 - \dot{y}_2 - \dot{y}_0) + d\dot{y}_1 + k_1(2y_1 - y_2 - y_0) + k_2(2\dot{y}_1 - \dot{y}_2 - \dot{y}_0)^3 = 0, \quad (1)$$

$$m_1\ddot{y}_2 + c(\dot{y}_2 - \dot{y}_1) + d\dot{y}_2 + k_1(\dot{y}_2 - \dot{y}_1) + k_2(\dot{y}_2 - \dot{y}_1)^3 = T\dot{q} + m_0 r \ddot{\phi} \cos \phi - m_0 r \dot{\phi}^2 \sin \phi, \quad (2)$$

$$m_0 r \ddot{y}_2 \cos \phi = I \ddot{\phi} + a \dot{\phi} - b, \quad (3)$$

$$T(\dot{y}_2 - \dot{y}_1) = -L\ddot{q} + R(1 - i_0^{-2}\dot{q}^2)\dot{q} - C_0^{-1}q - i_0^2\alpha_3 q^3 - i_0^4\alpha_5 q^5, \quad (4)$$

$$y_0 = f(t). \quad (5)$$

where y_j is the displacement of j^{th} story, $j=1,2$, m the mass of each story, c the interfloor damping (internal damping), d the external damping constant (velocity damping), k_1 the linear spring constant, k_2 the cubic spring constant, ϕ the angular displacement of the rotor, r the eccentricity of unbalanced shaft of the electric motor, $m_1 = m + m_0$ with m_0 the mass of unbalanced shaft of the electric motor, I the moment of inertia of the rotor, $T = 2\pi n l B$ the transducer constant, n the number of turns in the coil, l the radius of the coil, B the uniform radial magnetic field strength in the annular gap, L the inductor, C the capacitor, R the resistor, V_{res} the voltage in the resistor, V_{cond} the voltage in the capacitor, i_0 the initial current in the electrical part, C_0 the capacitive characteristic, α_3, α_5 the capacitor coefficients and q the instantaneous electrical charge.

The expression for the driving torque of the motor is $b - a\dot{\phi}$ (linear in the stationary regime) with b related to the voltage applied across to the armature of the DC motor, and a is a constant depending of the considered motor.

The electric component of the controller is composed by an inductor L , a capacitor C , and a resistor R . The expression of the voltage in resistor and the capacitor are [14]

$$V_{res} = -Ri_0 \left(\frac{\dot{q}}{i_0} - \frac{1}{3} \left(\frac{\dot{q}}{i_0} \right)^3 \right), \quad V_{cond} = \frac{q}{C_0} + \alpha_3 q^3 + \alpha_5 q^5, \quad (6)$$

In (2) the right side term represents the action of the source of energy. Eq. (3) expresses the supplying of the last story with the source energy. Eqs. (4) and (5) represent the boundary conditions for Eqs. (1)-(3).

When loading is deterministic, the function $f(t)$ is known as a function of time. When loading is random, the function $f(t)$ is not known a priori and it is defined statistically. The function $f(t)$ can be viewed as the harmonic excitation

$$f(t) = f_0 \sin \Omega t, \quad 0 \leq t \leq T, \quad (7)$$

with Ω a constant, or the step dependent function $\Omega(t)$

$$\Omega(t) = \omega_1 \left[1 + \frac{\omega_2 - \omega_1}{2\omega_1} \left(1 + \frac{1}{2} \tanh(\varepsilon(t - t_s)) \right) \right], \quad 0 \leq t \leq T, \quad (8)$$

where ω_1 and ω_2 the initial and final frequencies, t_s is the time at which the frequency is changed, and $\varepsilon \rightarrow \infty$ is a parameter which describes the step function limit [24].

In the second part of this article, the function $f(t)$ can be viewed as an average of various data y_0 measured from k^{th} earth motions $y_0 = f_k(t)$. This is equivalent to obtain $f_k(t)$ from the average curve $E\{f(t)\}$. The earthquakes are of short duration, so the process is not stationary. From this point of view we can not use a purely random stationary Gaussian process.

Eqs. (1)-(5) and (7) are written in a dimensionless version as

$$x_1'' + \beta_1 x_1' + A(\alpha + \delta_1 A^2) = 0, \quad A = 2x_1' - x_2' - x_0', \quad (9)$$

$$x_2'' + \beta_1 \mu x_2' - \lambda_1 x_4' + B\mu(\alpha + \delta_1 B^2) = (1 - \mu)(x_3'' \cos x_3 - x_3'^2 \sin x_3), \quad B = x_2' - x_1', \quad (10)$$

$$x_3'' - \eta_1 x_2'' \cos x_3 + u x_3' = v, \quad (11)$$

$$x_4'' - \alpha_2 x_4' + \beta_2 x_4'^3 + \gamma_2 x_4 + \delta_2 x_4^3 + \eta_2 x_4^5 + \lambda_2 B = 0, \quad (12)$$

$$x_0 = g(\vartheta), \quad (13)$$

where prime means the differentiation with respect to τ , and

$$\begin{aligned} \tau = \omega_1 t, \quad x_0 = \frac{y_0}{r}, \quad x_1 = \frac{y_1}{r}, \quad x_2 = \frac{y_2}{r}, \quad x_3 = \varphi, \quad x_4 = \frac{q}{q_0}, \quad \mu = \frac{m}{m + m_0} = \frac{m}{m_1}, \\ \alpha_1 = \frac{c}{m\omega_1}, \quad \beta_1 = \frac{d}{m\omega_1}, \quad \alpha = \alpha_1 + \gamma_1, \quad \gamma_1 = \frac{k_1}{m\omega_1}, \quad \delta_1 = \frac{k_2 r^2 \omega_1}{m}, \\ \lambda_1 = \frac{Tq_0}{m_1 r \omega_1}, \quad \eta_1 = \frac{rm_0}{I}, \quad u = \frac{a}{I\omega_1}, \quad v = \frac{b}{I\omega_1^2}, \\ \lambda_2 = \frac{Tr}{q_0 L \omega_1}, \quad \alpha_2 = \frac{R}{L\omega_1}, \quad \beta_2 = \frac{Rq_0^2 \omega_1}{i_0^2 L}, \quad \gamma_2 = \frac{1}{LC_0 \omega_1^2}, \\ \delta_2 = \frac{i_0^2 \alpha_3 q_0^2}{L\omega_1^2}, \quad \eta_2 = \frac{i_0^4 \alpha_5 q_0^4}{L\omega_1^2}, \quad \vartheta = \frac{\Omega}{\omega_1}. \end{aligned} \quad (14)$$

In (14) ω_1 is the first natural frequency of the structure. The unknowns of Eqs.(9)-(13) are the dimensionless displacement of j^{th} story x_j , $j = 1, 2$, the angular displacement of the rotor x_3 , and the dimensionless instantaneous electrical charge x_4 . The resonance condition with the building is given by $x_3' = 1$. In this case $\dot{\varphi} = \omega_1 \varphi' = \omega_1$. The first control parameter is μ which is the ratio between the mass of each story m and $m_1 = m + m_0$, with m_0 the mass of unbalanced shaft of the electric motor. The second control parameter is $v = \frac{b}{I\omega_1^2}$ where b is related to voltage applied across to the DC motor, I is the moment of inertia of the rotor and ω_1 is the first natural frequency of the structure.

In the case of (7), the equation (13) becomes

$$x_0 = g_0 \sin(\tau\vartheta), \quad 0 \leq \tau \leq T_\tau, \quad T_\tau = \omega_1 T, \quad g_0 = \frac{f_0}{r}. \quad (15)$$

In the case of (8), the equation (13) becomes

$$x_0 = g_0 \sin(\tau\vartheta(\tau)), \quad 0 \leq \tau \leq T_\tau, \quad T_\tau = \omega_1 T, \quad g_0 = \frac{f_0}{r}, \quad (16)$$

with

$$\vartheta(\tau) = 1 + \frac{\omega_2 - \omega_1}{2\omega_1} \left(1 + \frac{1}{2} \tanh(\varepsilon_s(\tau - \tau_s)) \right), \quad (17)$$

and

$$\tau_s = \omega_1 t_s, \quad \varepsilon_s = \frac{\varepsilon}{\omega_1}. \quad (18)$$

3 SOLUTIONS

The general solution of the system (9)-(13) may be written in the terms of the *theta function* representation

$$\theta(t) = \frac{d^2}{dt^2} \log \Theta_n(\eta_1, \eta_2, \dots, \eta_n), \quad (19)$$

where Θ is the *theta function* defined as

$$\Theta_n(\eta_1, \eta_2, \dots, \eta_n) = \sum_{M \in (-\infty, \infty)} \exp \left(i \sum_{i=1}^n M_i \eta_i + \frac{1}{2} \sum_{i,j=1}^n M_i B_{ij} M_j \right), \quad (20)$$

with n the number of degrees of freedom for a particular solutions, and

$$\eta_j = -\tilde{\omega}_j t + \phi_j, \quad 1 \leq j \leq N. \quad (21)$$

In (21), $\tilde{\omega}_j$ are the frequencies and the ϕ_j the phases. Also, we can write

$$M\eta = -\tilde{\Omega}t + \Phi, \quad M = [M_1, M_2, \dots, M_n], \quad \tilde{\Omega} = M\tilde{\omega}, \quad \Phi = M\phi.$$

The integer components in M are the integer indices in (16). The matrix B can be decomposed in a diagonal matrix D and an off-diagonal matrix O , that is $B = D + O$.

The solution (19) of Eqs. (9)-(13) can be written as [23]

$$\theta(t) = \frac{2}{\lambda} \frac{\partial^2}{\partial t^2} \log \Theta_n(\eta) = \theta_{lin}(\eta) + \theta_{int}(\eta), \quad (22)$$

where θ_{lin} represents a linear superposition of cnoidal vibrations

$$\theta_{lin}(\eta) = \frac{2}{\lambda} \frac{\partial^2}{\partial t^2} \log G(\eta), \quad G(\eta) = \sum_M \exp \left(iM\eta + \frac{1}{2} M^T D M \right), \quad (23)$$

and θ_{int} represents a nonlinear interaction among the cnoidal vibrations

$$\theta_{int}(\eta) = 2 \frac{\partial^2}{\partial t^2} \log \left(1 + \frac{F(\eta, C)}{G(\eta)} \right), \quad F(\eta, C) = \sum_{M^\alpha} C \exp(iM\eta + \frac{1}{2} M^T D M),$$

$$C = \exp(\frac{1}{2} M^T O M) - 1. \quad (24)$$

The first term θ_{lin} represents, as above, a linear superposition of cnoidal waves. Indeed, after a little manipulation and algebraic calculus, (19) gives

$$\theta_{lin} = \sum_{l=1}^n \alpha_l \left[\frac{2\pi}{\tilde{K}_l \sqrt{m_l}} \sum_{k=0}^{\infty} \left(\frac{q_l^{k+1/2}}{1+q_l^{2k+1}} \cos(2k+1) \frac{\pi \tilde{\omega}_l t}{2\tilde{K}_l} \right)^2 \right], \quad (25)$$

with

$$q = \exp(-\pi \frac{K'}{K}), \quad \tilde{K} = \tilde{K}(\tilde{m}) + \int_0^{\pi/2} \frac{du}{\sqrt{1-\tilde{m} \sin^2 u}}, \quad \tilde{K}'(\tilde{m}_1) = \tilde{K}(\tilde{m}), \quad \tilde{m} + \tilde{m}_1 = 1.$$

In (25) we recognize the expression [25]

$$\theta_{lin} = \int_{-\infty}^{\infty} \alpha \text{cn}^2[\tilde{\omega}t; \tilde{m}] dt, \quad (26)$$

The second term θ_{int} represents a nonlinear superposition or interaction among cnoidal waves. We write this term as [23]

$$2 \frac{d^2}{dt^2} \log \left[1 + \frac{F(t)}{G(t)} \right] \approx \frac{\beta \text{cn}^2(\tilde{\omega}t, \tilde{m})}{1 + \gamma \text{cn}^2(\tilde{\omega}t, \tilde{m})}. \quad (27)$$

If \tilde{m} take the values 0 or 1, the relation (27) is directly verified. For $0 \leq \tilde{m} \leq 1$, the relation is numerically verified with an error of $|e| \leq 5 \times 10^{-7}$. Consequently, we have in the general case

$$\theta_{int}(t) = \int_{-\infty}^{\infty} \frac{\tilde{\beta} \text{cn}^2[\tilde{\omega}t; \tilde{m}]}{1 + \tilde{\gamma} \text{cn}^2[\tilde{\omega}t; \tilde{m}]} dt. \quad (28)$$

As a result, the cnoidal method yields to solutions consisting of a linear superposition and a nonlinear superposition of cnoidal vibrations.

In the general case, the solution of the problem (9)-(13) can be written as

$$x_j(t) = \int_{-\infty}^{\infty} K_j(t) g(t-\tau) d\tau = \int_{-\infty}^{\infty} K_j(t-\tau) g(\tau) d\tau, \quad j=1, 2, \dots, 4 \quad (29)$$

where

$$K_j(t) = \sum_{k=1}^n \left[\text{cn}^2[\tilde{\omega}_{jk}t; \tilde{m}_{jk}] + \frac{\tilde{\beta}_{jk} \text{cn}^2(\tilde{\omega}_{jk}t, \tilde{m}_{jk})}{1 + \tilde{\gamma}_{jk} \text{cn}^2(\tilde{\omega}_{jk}t, \tilde{m}_{jk})} \right], \quad j=1, 2, \dots, 4. \quad (30)$$

The solution (29) requires the evaluation of unknowns $\tilde{\omega}$, \tilde{m} , $\tilde{\beta}$ and $\tilde{\gamma}$. Substitution of (29) into Eqs. (9)-(13) gives a set of identities from which the parameters can be evaluated. The

identities results by equating the coefficients for expression terms containing the functions cn and sn in the same power.

4 CONSTANT EXCITATION FREQUENCY

The solutions (27) and (28) are computed for $n=7$ degrees of freedom for particular solutions and for different values of the parameters of the system and a constant excitation frequency Ω .

Before discussing the results of the numerical calculations, we briefly explain the choice of the control model parameters. Firstly, the range of μ varies from 0.7 to 1. The value $\mu=0.7$ corresponds to the case when the m_0 represents 40% of m , while $\mu=1$ means that the m_0 is negligible compared to m .

The decreasing of the control parameter v with respect to time in the transition interval ($\phi'=0$) is represented in Fig. 2. The time frames are the following: $0 \leq \tau \leq 500$ and $500 \leq \tau \leq 800$ above the resonance, $800 \leq \tau \leq 1400$ inside resonance, and $1400 \leq \tau \leq 1600$, $1600 \leq \tau \leq 2000$ below the resonance, respectively. The parameter values were selected as $\mu=0.7$, $\alpha_1=$, $\beta_1=$, $\gamma_1=$, $\delta_1=$, $\lambda_1=$, $\eta_1=$, $u=$, $\lambda_2=$, $\alpha_2=$, $\beta_2=$, $\gamma_2=$, $\delta_2=$, $\eta_2=$ and $\vartheta=1$.

The time variation of the displacement x_1 corresponding to the last story without/with the electromechanical vibration absorber, are plotted in Figures 3 and 4, respectively, during the transition through the resonance region.

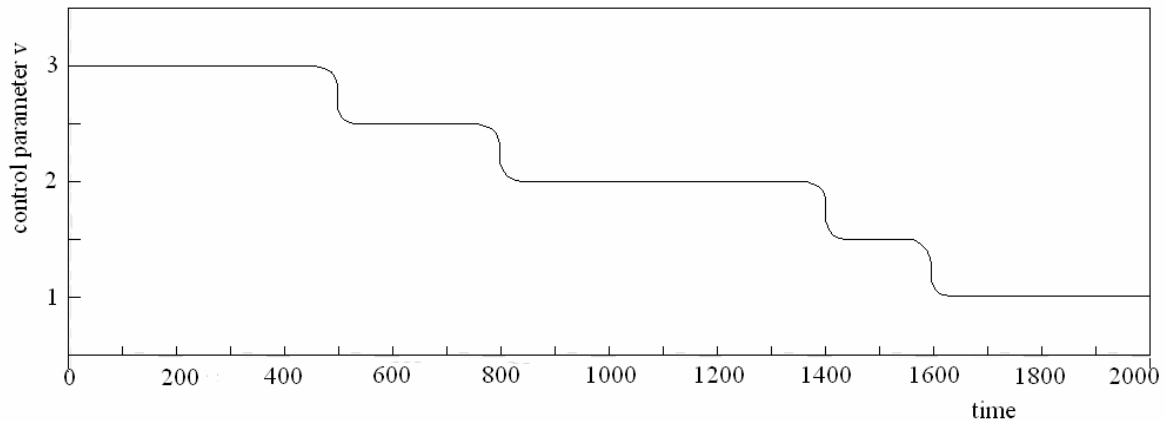


Figure 2. The decreasing of the control parameter v with respect to time in the transition interval.

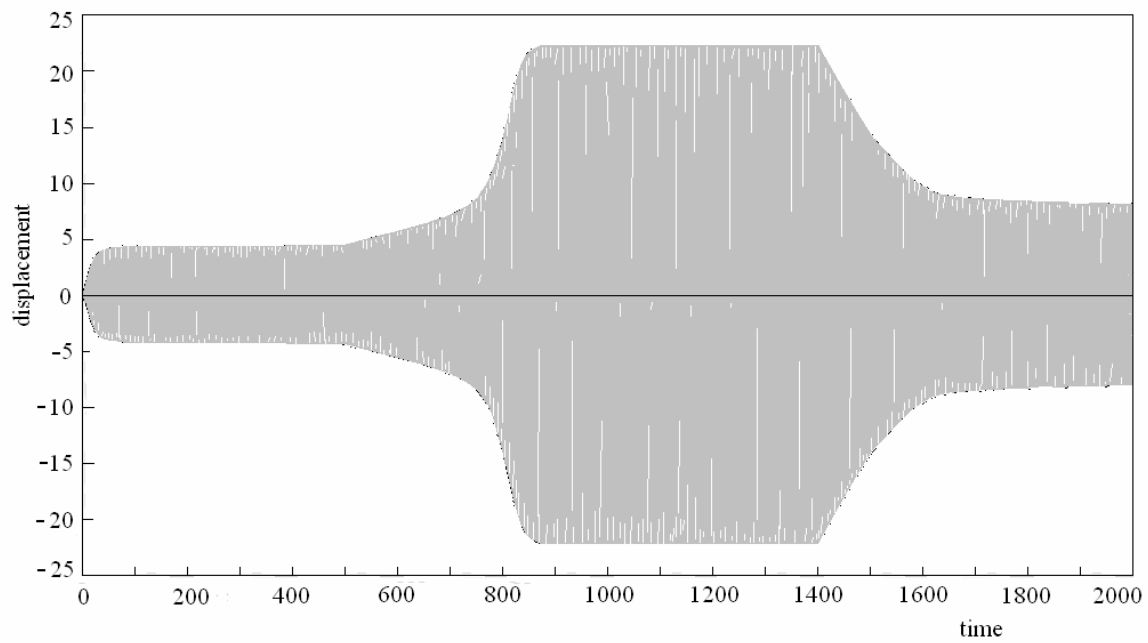


Figure 3. Time history for the last story without the electromechanical vibration absorber.

The time variation of the angular velocity x_3 of the DC motor without/with the electromechanical vibration absorber, are simulated in Figures 3 and 4, respectively, during the transition through the resonance region.

Figure 3 shows that in the case of no coupling between the electromechanical vibration absorber and the structure, the vibration amplitude increase in the time range $800 \leq \tau \leq 1400$ inside resonance, while Figure 4 shows that in the case of coupling, the vibration amplitude significantly reduce in time ranges $800 \leq \tau \leq 1400$ inside resonance, and $1400 \leq \tau \leq 1600$, $1600 \leq \tau \leq 2000$ below the resonance.

In Figure 5, the capture of the resonance of the angular velocity is put into evidence in the case of no coupling. Fig.6 shows that in the case of coupling, the Sommerfeld effect cancels the resonance of the angular velocity and reduces significantly the vibration amplitudes.

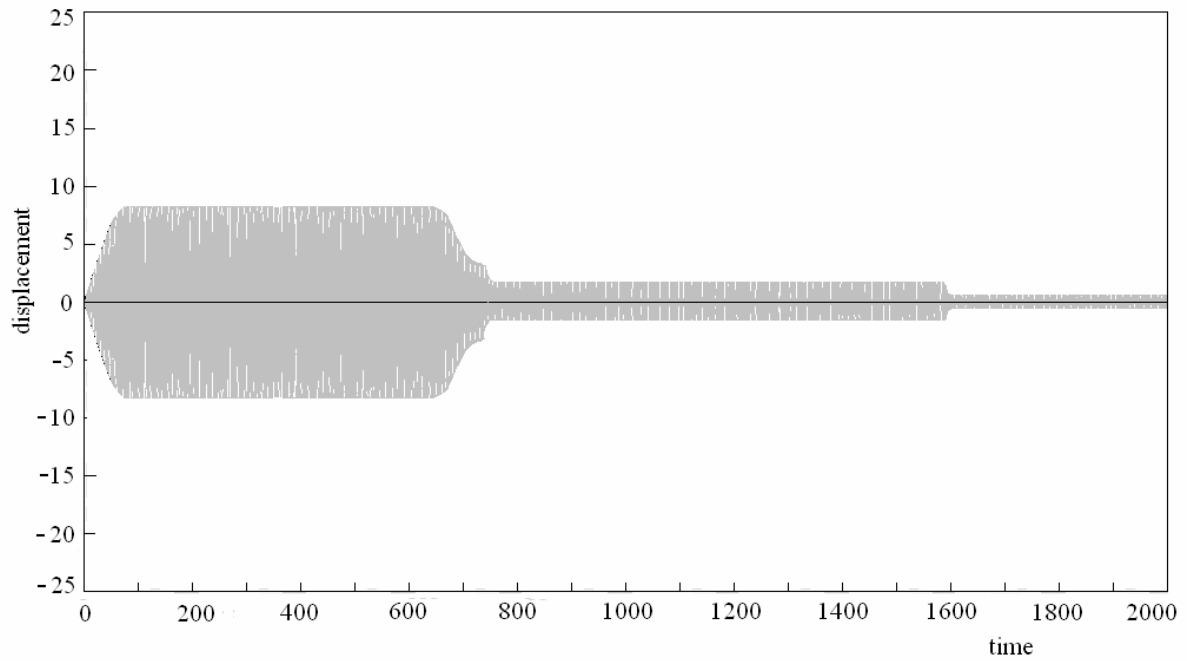


Figure 4. Time history for the last story with the electromechanical vibration absorber.

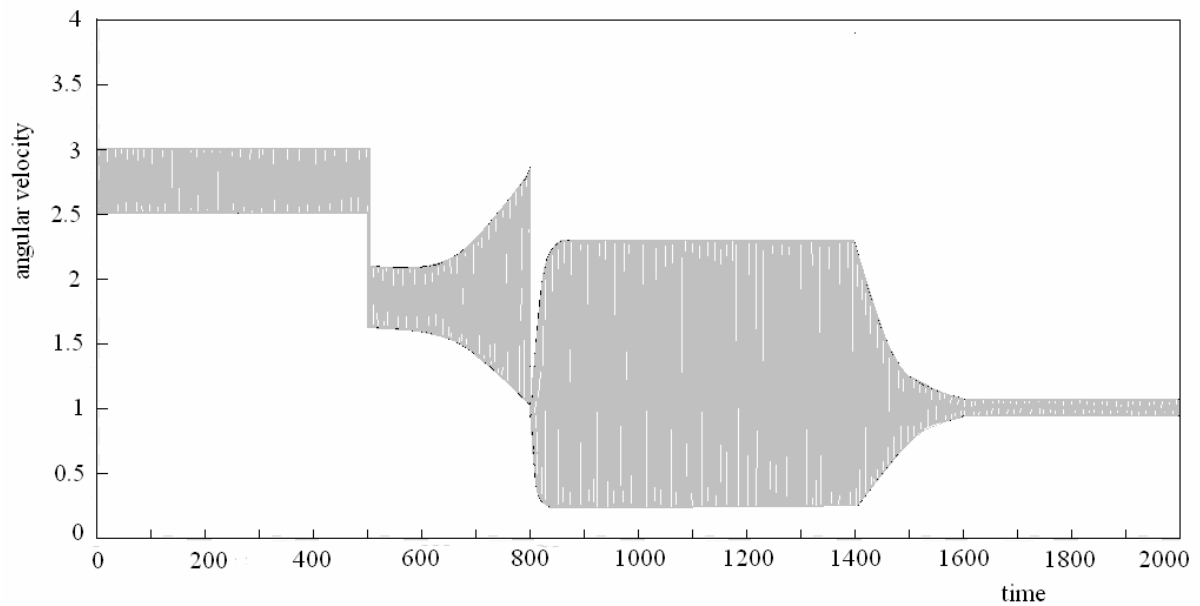


Figure 5. Time history for the angular velocity of the DC motor without the electromechanical vibration absorber.

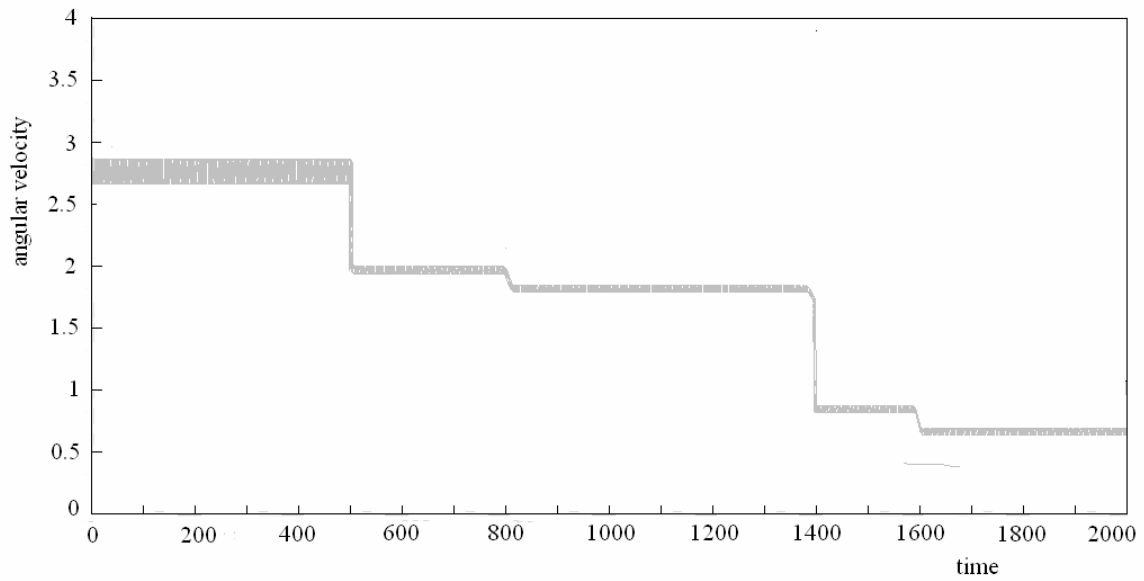


Figure 6. Time history for the angular velocity of the DC motor with the electromechanical vibration absorber.

5 CASE OF THE TIME-DEPENDENT EXCITATION FREQUENCY

The step function (8) is introduced for two cases: (1) $t = 2$ in the interval $0 \leq \tau \leq 500$ above the resonance and (2) $t = 815$ in the interval $800 \leq \tau \leq 1400$ inside the resonance. Fig. 7 plots, for example, the step function (9) in the interval $0 \leq \tau \leq 500$ for $\omega_1 = 1$ and $\omega_2 = 2$ (solid line) and $\omega_2 = 3$ (dash line) and $\varepsilon = 20$, $t_s = 2$. For other intervals, the step function has similar shapes.

In the case (1), the control parameter v knows a sudden variation with respect to time at the beginning of the interval as shown in Figure 8, for both the solid and dash lines, respectively. For $t > 60$, the control parameter is constant and then it jumps to the value 2.5 when $t = 500$.

Upon the matching of two time independent solutions at the time when the step occurs, we obtain the time variation of the displacement x_1 corresponding to the last story without/with the electromechanical vibration absorber, are plotted in Figures. 9 and 10, respectively, during the interval above the resonance, in the case of both solid and dash lines (blue and green contours), respectively. The displacements present squeezing and weaving, and reduction in magnitude for $t > 475$, according to Figure 9. Figure 10 exhibits also squeezing and weaving with increase of the magnitude for $t > 400$. The squeezing and amplitude are enhanced for the dash line (blue and green contours) in both figures. Numerical experiments showed that the squeezing may be enhanced by increasing the frequency difference $\omega_2 - \omega_1$.

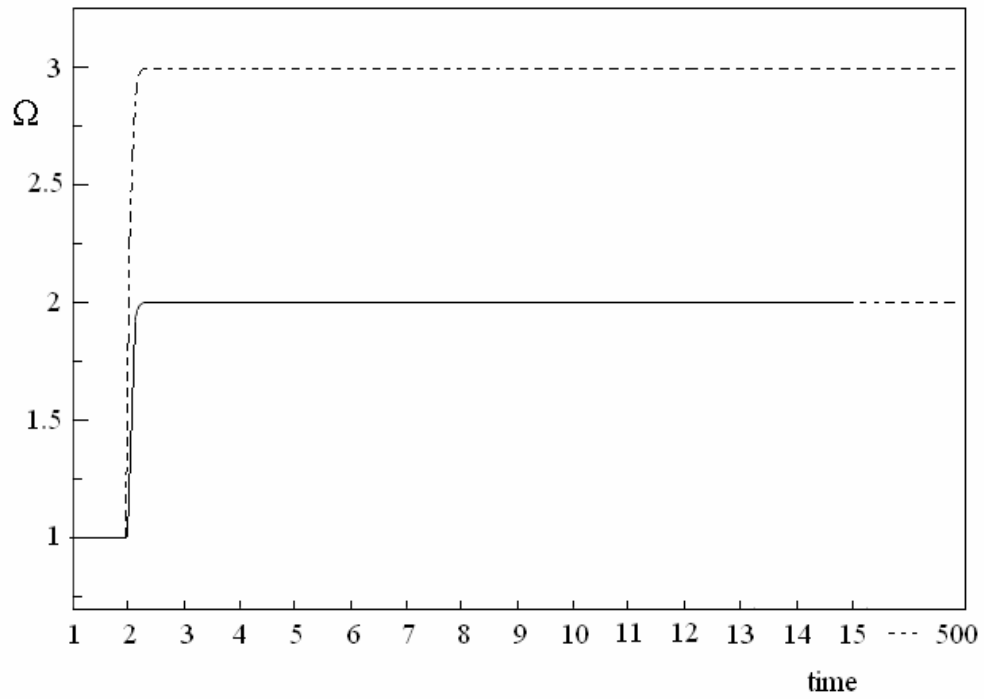


Figure 7. $\Omega(t)$ as a function of t in the interval above the resonance.

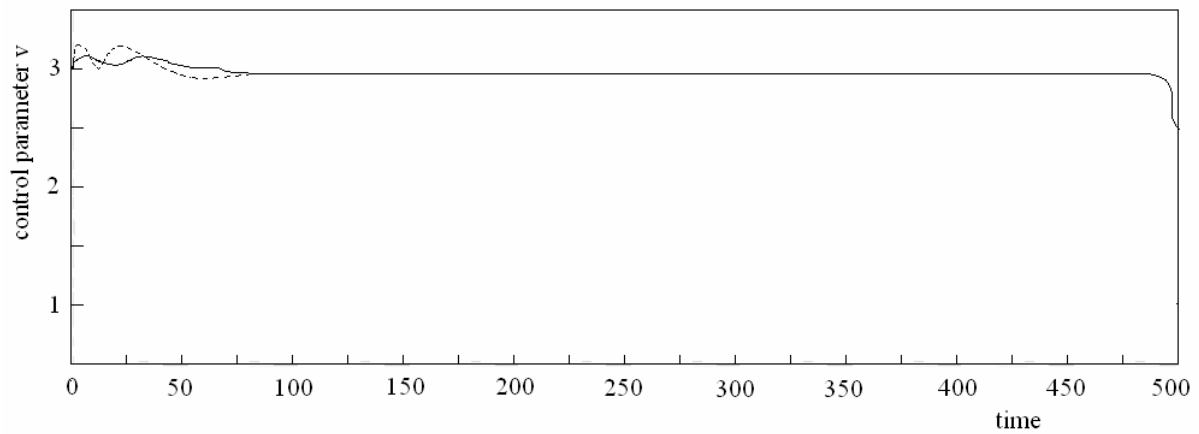


Figure 8. The variation of the control parameter v with respect to time in the interval above the resonance.

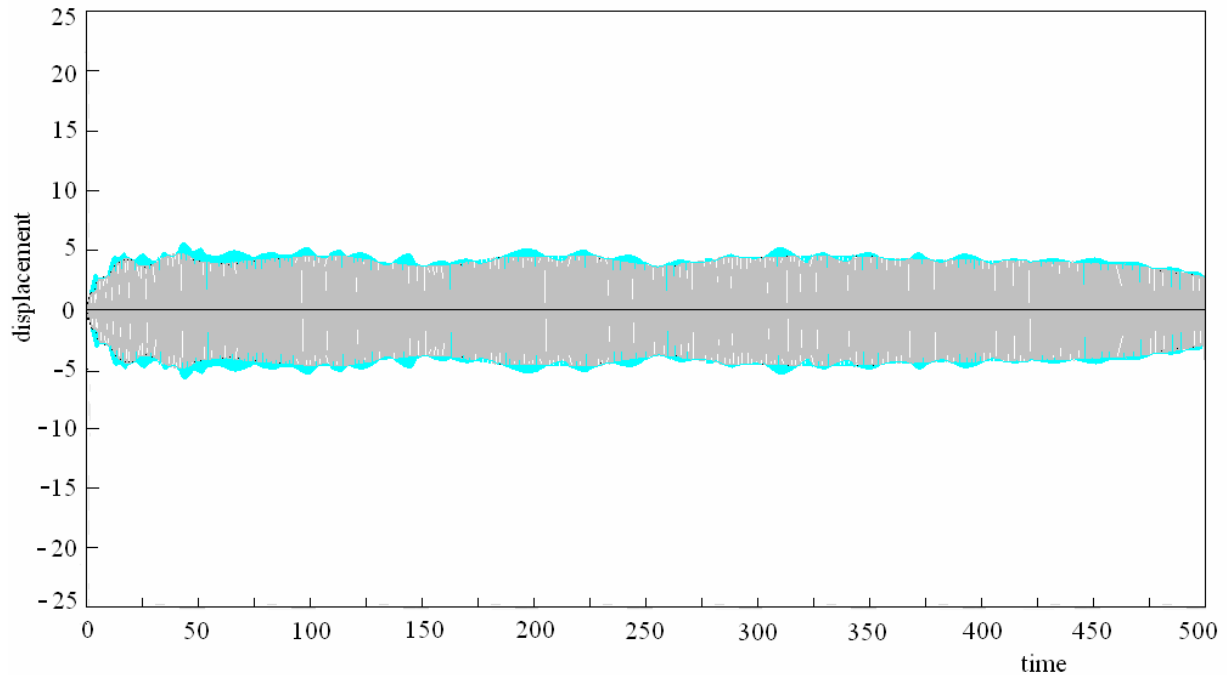


Figure 9. Time history for the last story without the electromechanical vibration absorber, during the interval above the resonance.

In the second case, the variation of the control parameter ν is shown in Figure 11. As in the previous case, the control parameter has sudden variations with respect to time at the beginning and at the end of the interval, respectively, for both the solid and dash lines. For $900 < t < 1315$, the control parameter is constant and then it jumps to the value 1.5 when $t = 1400$. The time variation of the displacement x_1 corresponding to the last story without/with the electromechanical vibration absorber, are plotted in Figures 12 and 13, respectively, during the interval inside the resonance, in the case of both solid and dash lines (blue and green contours), respectively. The displacements present squeezing and weaving, and an increasing in magnitude for the last story without the electromechanical vibration absorber, inside the resonance, according to Figure 12.

The squeezing and amplitude are enhanced for the dash line (blue and green contours) in Figure 12. Figure 13 exhibits also squeezing and weaving with a substantial decrease of the magnitude for the last story with the electromechanical vibration absorber, inside the resonance.

As a conclusion, by comparing Figure 4 with Figure 13 which presents the history for the last story with the electromechanical vibration absorber for the constant excitation frequency and the time-dependent excitation frequency, respectively, we see that the control system efficiency is higher in the last case.

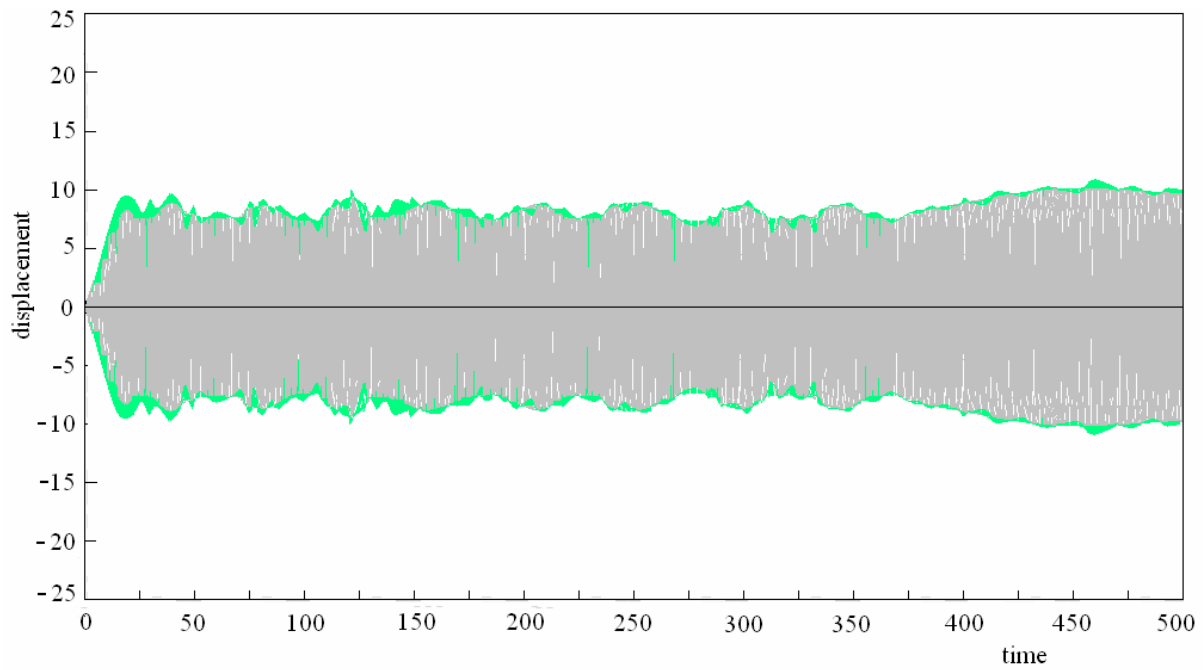


Figure 10. Time history for the last story with the electromechanical vibration absorber, during the interval above the resonance. The green contour corresponds to the dash line.

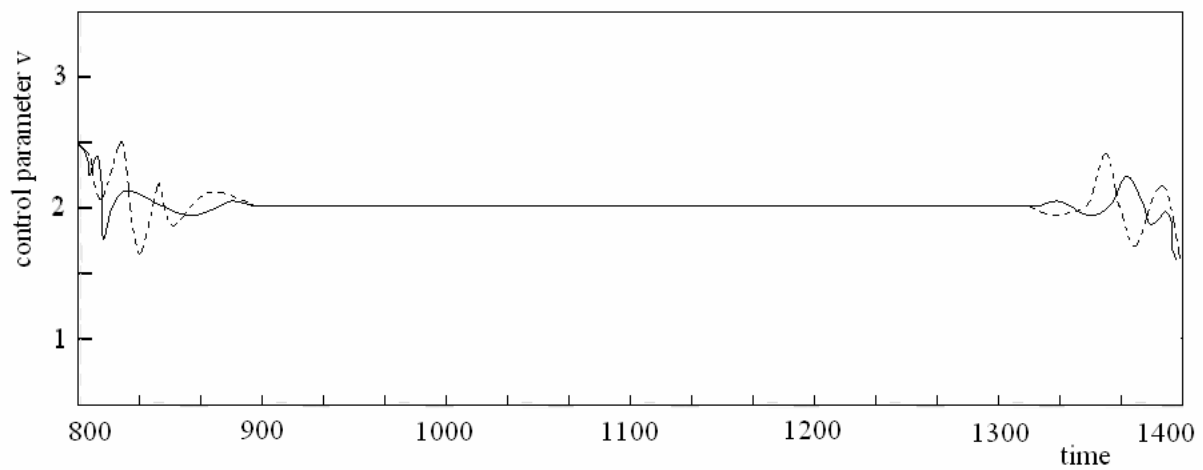


Figure 11. The variation of the control parameter v with respect to time in the interval inside the resonance.

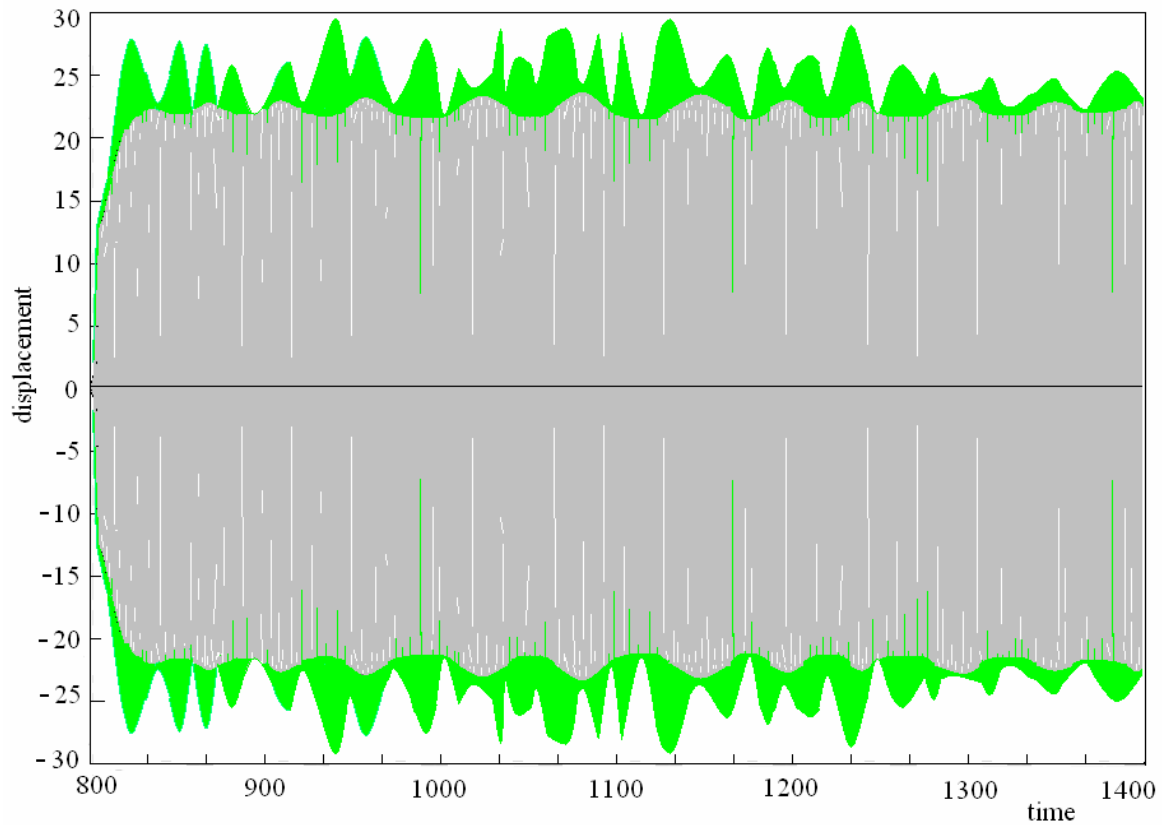


Figure 12. Time history for the last story without the electromechanical vibration absorber, during the interval inside the resonance. The green contour corresponds to the dash line.

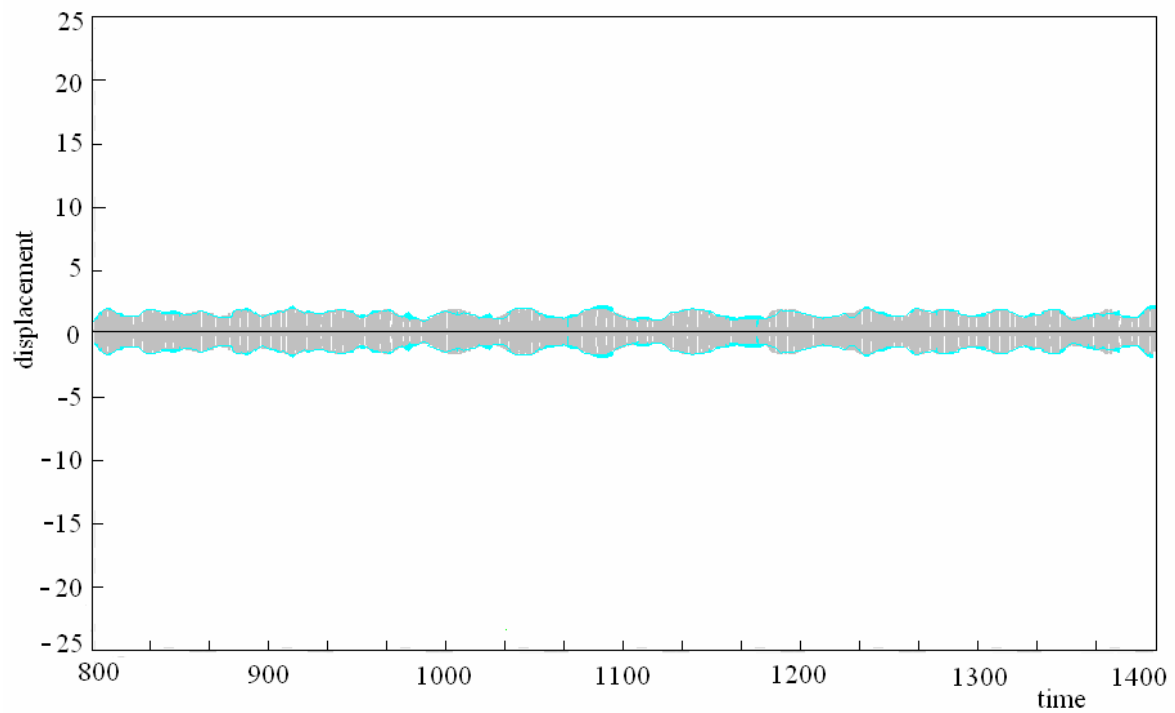


Figure 13. Time history for the last story with the electromechanical vibration absorber, during the interval inside the resonance. The green contour corresponds to the dash line.

6 CASE OF THE RANDOM EARTHQUAKES

In this Section, the function $f(t)$ is viewed as an average of various data y_0 measured from k^{th} earth motions $y_0 = f_k(t)$. This is equivalent to obtain $f_k(t)$ from the average curve $E\{f(t)\}$. The earthquakes are of short duration, so the process is not stationary. From this point of view we can not use a purely random stationary Gaussian process.

We start with 1D expected value $E\{f(t)\}$, and the 2D expected function $E\{f(t_1), f(t_2)\}$ respectively, which are given by [6]

$$\begin{aligned} E\{f(t)\} &= \int_{-\infty}^{\infty} f(t)W_1(f(t))df(t), \\ E\{f(t_1)f(t_2)\} &= \int_{-\infty}^{\infty} f(t_1)f(t_2)W_2(f(t_1), f(t_2))df(t_1)df(t_2), \end{aligned} \quad (31)$$

where $W_1(f)$ and $W_2(f(t_1), f(t_2))$ are the 1D probability density function for a given t , and the 2D probability density function, respectively, for given t_1 and t_2 . The n^{th} and m^{th} moments ($m, n = 0, 1, 2, \dots$) are also calculated

$$E\{f^n(t)\} = \int_{-\infty}^{\infty} f^n(t)W_1(f)df, \quad E\{f^m(t_1)f^n(t_2)\} = \int_{-\infty}^{\infty} f^m(t_1)f^n(t_2)W_2(f^m(t_1), f^n(t_2))df. \quad (32)$$

For $m = n = 1$, the correlation function $R_f(t_1, t_2)$ is obtained

$$R_f(t_1, t_2) = E\{f(t_1)f(t_2)\} = \int_{-\infty}^{\infty} f(t_1)f(t_2)W_2(f(t_1), f(t_2))df(t_1)df(t_2). \quad (33)$$

In (7) we can change $f(t)$ with $E\{f(t)\}$ or $R_f(t_1, t_2) = E\{f(t_1), f(t_2)\}$ so that the calculations to remain the same as in the deterministic case. If the correlation function $R_f(t_1, t_2)$ is known, we can calculate the cross correlation functions

$$R_{y_j y_k}(t_1, t_2) = E\{y_j(t_1)y_k(t_2)\} = \int_{-\infty}^{\infty} y_j(t_1)y_k(t_2)W_2(y_j(t_1), y_k(t_2))dy_j(t_1)dy_k(t_2), \quad (34)$$

and the square displacements $E\{y_j^2(t)\}$ for the j^{th} , $j = 1, 2$ story

$$E\{y_j^2(t)\} = \int_{-\infty}^{\infty} y_j^2(t)W_2(y_j(t), y_j(t))dy(t). \quad (35)$$

The solution (29) allows the calculating of various averages

$$E\{y_j(t)\} = \int_{-\infty}^t K_j(t - \tau)E\{f(\tau)\}d\tau, \quad (36)$$

$$E\{y_j(t_1)y_k(t_2)\} = \int_{-\infty}^{t_1} \int_{-\infty}^{t_2} K_j(t_1 - \tau_1)K_k(t_2 - \tau_2)E\{f(\tau_1)f(\tau_2)\}d\tau_1d\tau_2, \quad (37)$$

When $E\{f(\tau)\} = 0$, from (36) it results $E\{y_j(t)\} = 0$. If the autocorrelation function of $f(t)$ is known, we see from (10) that $R_f(t_1, t_2)$ is also known. So, we obtain from (37)

$$R_{y_j y_k} = \int_{-\infty}^{t_1} \int_{-\infty}^{t_2} K_j(t_1 - \tau_1)K_k(t_2 - \tau_2)R_f(\tau_1, \tau_2)d\tau_1d\tau_2. \quad (38)$$

Calculation of the mean kinetic energy for each story requires the calculation of the integral

$$R_{\dot{y}_j \dot{y}_k} = \int_{-\infty}^{t_1} \int_{-\infty}^{t_2} \dot{K}_j(t_1 - \tau_1)\dot{K}_k(t_2 - \tau_2)\dot{R}_f(\tau_1, \tau_2)d\tau_1d\tau_2. \quad (39)$$

The shearing force correlation includes the part given by the spring force and the part that is dissipated by the internal damping

$$V_1 = c(2\dot{y}_1 - \dot{y}_2 - \dot{y}_0) + k_1(2\dot{y}_1 - \dot{y}_2 - \dot{y}_0) + k_2(2\dot{y}_1 - \dot{y}_2 - \dot{y}_0)^3,$$

$$V_2 = c(\dot{y}_2 - \dot{y}_1) + k_1(\dot{y}_2 - \dot{y}_1) + k_2(\dot{y}_2 - \dot{y}_1)^3.$$

The expression for the shearing force correlation is

$$R_{V_j V_k}(t_1, t_2) = \int_{-\infty}^{t_1} \int_{-\infty}^{t_2} K_j(t_1 - \tau_1)K_k(t_2 - \tau_2)R_{V_j V_k}(\tau_1, \tau_2)d\tau_1d\tau_2, \quad (40)$$

where $R_{V_j V_k}(t_1, t_2) = R_{j,k} - R_{j,k-1}$.

The 1D and 2D probability density functions are given by [6]

$$W_1(y_j) = \frac{1}{\sigma_j \sqrt{2\pi}} \exp\left(\frac{-y_j^2}{2\sigma_j^2}\right), \quad (41)$$

$$W_2(y_j, y_k) = \frac{1}{\sigma_j \tau_k \sqrt{2\pi(1-\rho_{jk})}} \exp\left[\frac{1}{(1-\sigma_{jk})} \left(-\frac{y_j^2}{2\sigma_j^2} - \frac{y_k^2}{2\tau_k^2} + \frac{2\rho_{jk}y_j y_k}{\sigma_j \tau_k}\right)\right], \quad (42)$$

with

$$\sigma_j^2 = E\{y_j^2\} - E^2\{y_j\} = R_{y_j}(t, t), \quad \sigma_{jk} = \sigma_j \tau_k R_{y_j y_k}(t, t), \quad \tau_k^2 = R_{y_k}(t, t). \quad (43)$$

With (41) or (42), the correlation functions and various moments can be calculated

$$E\{y_j\} = \int_{-\infty}^{\infty} y_j W_1(y_j) dy_j, \quad E\{y_j y_k\} = \int_{-\infty}^{\infty} \int_{-\infty}^{\infty} y_j y_k W_2(y_j, y_k) dy_j dy_k = R_{y_j y_k}, \quad (44)$$

$$E\{y_j^n\} = \int_{-\infty}^{\infty} y_j^n W_1(y_j) dy_j, \quad E\{y_j^m y_k^n\} = \int_{-\infty}^{\infty} \int_{-\infty}^{\infty} y_j^m y_k^n W_2(y_j, y_k) dy_j dy_k. \quad (45)$$

The autocorrelation functions $R_{2,2}$, $R_{1,1}$ and the cross correlation functions $R_{1,2}$ respectively, are divided by $R_0 = \frac{4f_0^2}{441\pi^2}$, where f_0^2 is the spectral density (a constant) of R_f which characterizes a Gaussian processes, for which the correlation function $R_f(t_1, t_2)$ given by (10) becomes

$$R_f(t_1, t_2) = E\{f(t_1)f(t_2)\} = f_0^2 \delta(t_1 - t_2), \quad (46)$$

with $\delta(t)$ is the Dirac's delta function.

The autocorrelation functions $R_{2,2}$, $R_{1,1}$ and the cross correlation functions $R_{1,2}$ respectively, are plotted versus the correlation interval in Figs.14-16. The parameters values were selected as $R_0 = \frac{4f_0^2}{441\pi^2}$, $\frac{k}{m} = 50$, $c = d = 0.2$ [6], [14].

The autocorrelation function $R_{2,2}$ for the second story of the building is plotted versus the correlation interval in Fig.14, with and without the vibration absorber, respectively. The maximum displacement is observed at this story.

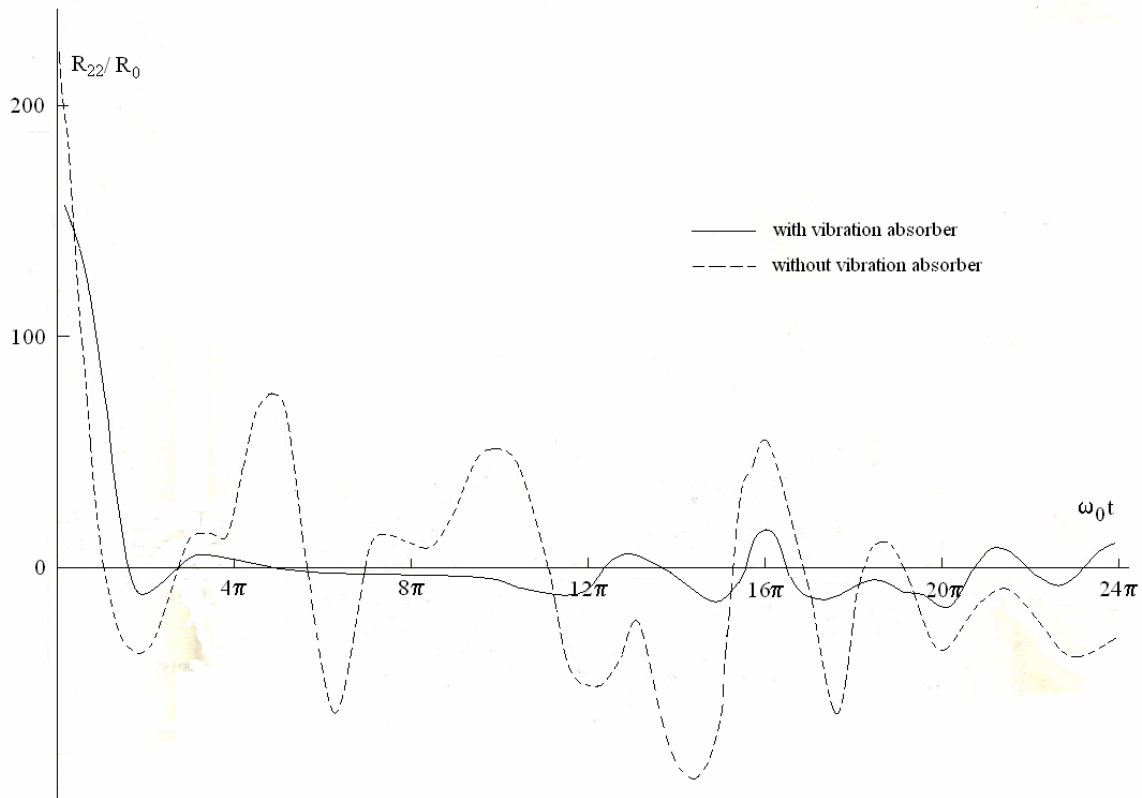


Figure 14. Displacement autocorrelation functions for the second story with and without the vibration absorber.

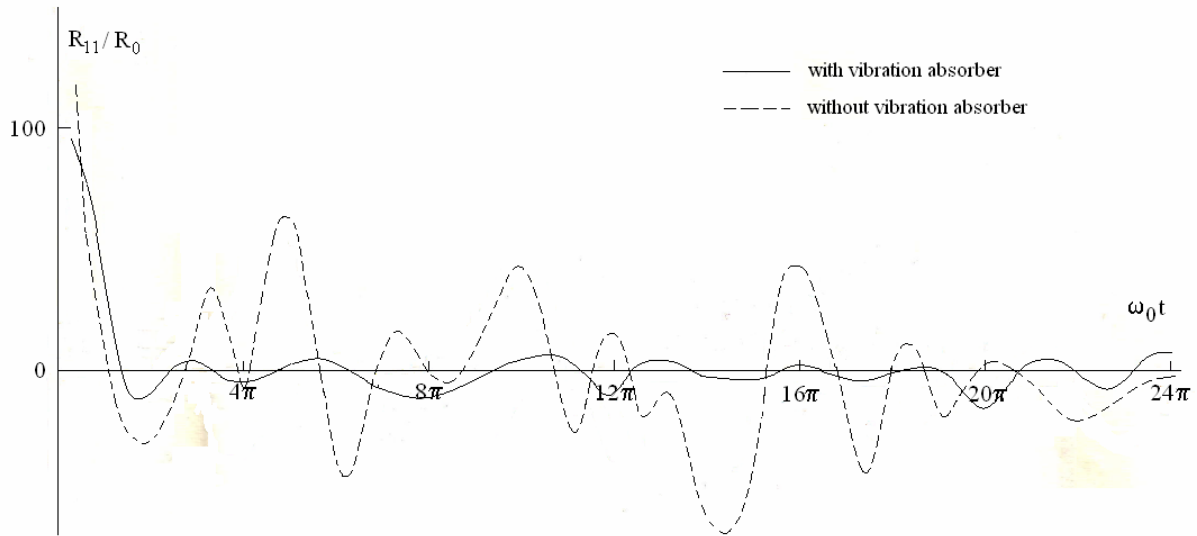


Figure 15. Displacement autocorrelation functions for the first story with and without the vibration absorber.

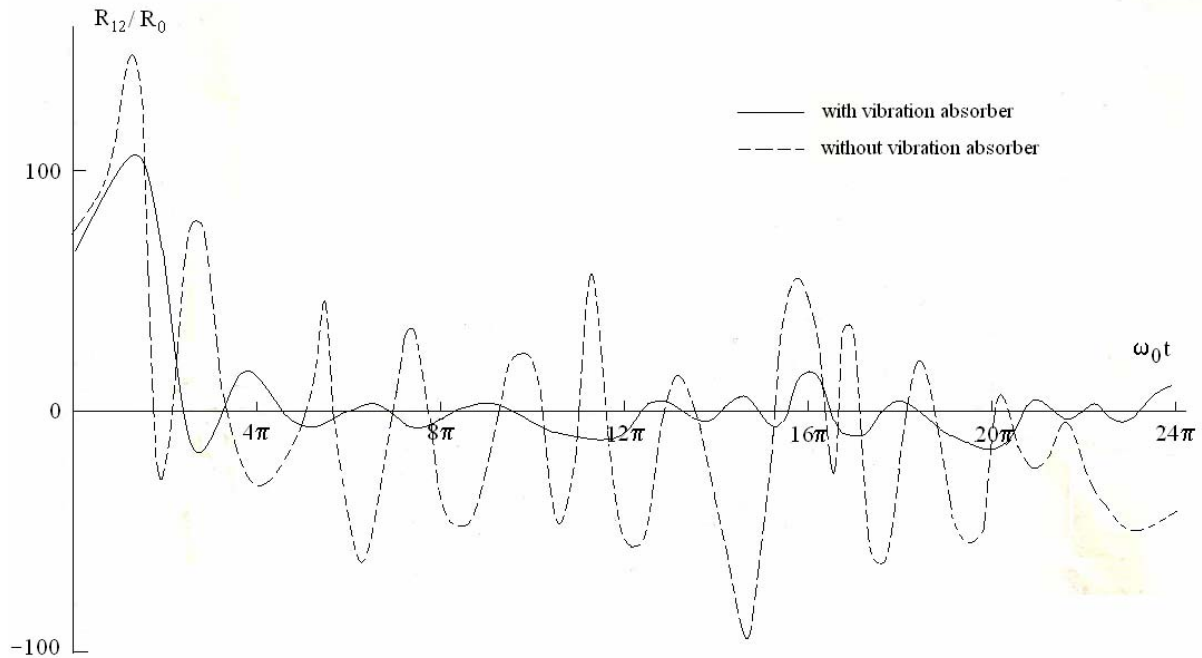


Figure 16. Displacement cross correlation functions with and without the vibration absorber.

7 CONCLUSIONS

This work is dealt with the analysis of the response to vibrations of a small building equipped with an electromechanical vibration absorber. The interaction between the vibrating system and the energy source is investigated for harmonic excitation with constant or step dependent frequencies, and for random earthquakes, respectively. This interaction corresponds to the systems with non-ideal excitation explained by the Sommerfeld effect which results from the balance of the energy and it is due to the coupling between the excitation mechanism and the vibrational loads. The resonance capture and the vibration reduction are displayed by the time history responses of the displacement and angular velocities above the resonance.

Since the earthquakes are of short duration, the stationary character is not available. Therefore, it is shown an attempt for calculation of the mean square displacements and cross correlation functions for this small building equipped with an electromechanical vibration absorber. Because of the stiffness nonlinearity, the equations cannot be solved by usually applied Fourier-integral type of solutions. The stochastic process which characterizes the earth movements is coupled to the cnoidal method which delivers the analytical solutions of the nonlinear problem.

Acknowledgement This research was elaborated through the PN-II-PT-PCCA-2011-3.1-0190 Project of the National Authority for Scientific Research (ANCS, UEFISCSU), contract 149/2012 Romania. The authors acknowledge the similar and equal contributions to this article. The corresponding author is Veturia Chiroiu.

REFERENCES

- [1] C.A. Cornell, Engineering Seismic Risk Analysis. *Bulletin of the Seismological Society of America*, **58**, 1583–1606, 1968.
- [2] G.H. Powell, R. Allahabadi, Seismic damage prediction by deterministic methods: Concepts and procedures. *Earthquake Engineering Structural Dynamics*, **16**(5), 719–734, 1988.
- [3] M. Radulian, G.F. Panza, M. Popa, B. Grecu, Seismic wave attenuation for Vrancea events revisited. *Journal of Earthquake Engineering*, **10**(3), 411–427, 2008.
- [4] F. Haas, J. Goedert, Dynamical systems and the Ermakov invariant. *Physics Letters A* **279**, 181, 2001.
- [5] S. Bouquet, H.R. Lewis, Extension of Giacomini's results concerning invariants for one-dimensional time dependent potentials. *Journal of Mathematical Physics*, **37**(11) 5496–5509, 1996.
- [6] A.C. Eringen, Response of tall buildings to random earthquakes. *Purdue University, Division of Engineering Sciences*, 1957.
- [7] M.C. Wang, G.E. Uhlenbeck, On the theory of the Brownian motion II. *Rev. Modern Phys.*, **17** (2), 323–342, 1945.
- [8] M.R. Spiegel, The random vibrations of a string. *Quarterly of Applied Mathematics* **10**(1), 1952.
- [9] J.L.P. Felix, J.M. Balthazar, R.M.L.R.F. Brasil, On saturation control of a nonideal vibrating portal frame foundation type shear-building. *Journal of Vibration and Control*, **11**, 121–136, 2005.
- [10] J.L.P. Felix, J.M. Balthazar, R.M.L.R.F. Brasil, On tuned liquid column dampers mounted on a structural frame under a nonideal excitation. *Journal of Sound and Vibration*, **282**, 1285–1292, 2005.
- [11] S.L.T. Souza, I.L. Caldas, R.L. Viana, J.M. Balthazar, J.M., R.M.L.R.F Brasil, Dynamics of vibrating systems with tuned liquid column dampers and limited power supply. *Journal of Sound and Vibration*, **289**, 987–998, 2006.

- [12] R.J. Nagem, S.I. Madanshetty, G. Medhi, An electromechanical vibration absorber. *Journal of Sound and Vibration*, **200**(4), 551–556, 1997.
- [13] M. Bolla, J.M. Balthazar, J.L.P. Felix, D.T. Mook, On an approximate analytical solution to a nonlinear vibrating problem, excited by a nonideal motor. *Nonlinear Dynamics*, **50**, 841–847, 2007.
- [14] J.L.P. Felix, J.M. Balthazar, Comments on a nonlinear and nonideal electromechanical damping vibration absorber. Sommerfeld effect and energy transfer. *Nonlinear Dynamics*, **55**, 1–11, 2009.
- [15] R. Yamapi, J.B. Chabi Orou, P. Wofo, Harmonic oscillations, stability and chaos control in a non-linear electromechanical system. *Journal of Sound and Vibration*, **259**(5), 1253–1264, 2003.
- [16] R. Yamapi, P. Wofo, Dynamics and synchronization of coupled self-sustained. *Journal of Sound and Vibration*, **285**, 1151–1170, 2005.
- [17] R. Yamapi, P. Wofo, Dynamics of an electromechanical damping device with magnetic coupling. *Communications in Nonlinear Science and Numerical Simulation*, **11**, 907–921, 2006.
- [18] G.S. Mbouna Ngueuteu, R. Yamapi, P. Wofo, Effects of higher nonlinearity on the dynamics and synchronization of two coupled electromechanical devices. *Communications in Nonlinear Science and Numerical Simulation*, **13**(6), 1121–1130, 2008.
- [19] J.M. Balthazar, B.I. Chesankov, D.T. Rushev, L. Barbanti, H.I. Weber, Remarks on the passage through resonance of a vibrating system with two degrees of freedom, excited by a nonideal energy source. *Journal of Sound and Vibration*, **239**(5), 1075– 1085, 2001.
- [20] J.M. Balthazar, D.T. Mook, H.I. Weber, R.M.L.R.F Brasil, A. Fenili, D. Belato, J.L.P. Felix, An overview on nonideal vibrations. *Meccanica*, **38**(6), 613–621, 2003.
- [21] K.V. Frolov, T.S. Krasnopolskaya, Sommerfeld effect in systems without internal damping. *International Applied Mechanics*, **23**(12), 1122–1126, 1987.
- [22] A.R. Osborne, Soliton physics and the periodic inverse scattering transform. *Physica D*, **86**, 81–89, 1995.
- [23] L. Munteanu, St. Donescu, *Introduction to Soliton Theory: Applications to Mechanics*. Book Series Fundamental Theories of Physics, vol.143, Kluwer Academic Publishers, Dordrecht, Boston (Springer Netherlands), 2004.
- [24] H. Moya-Cessa, M.F. Duasti, Coherent states for the time dependent harmonic oscillator: the step function. *Physics Letters A*, **311**, 1–5, 2003.
- [25] M.J. Ablowitz, H. Segur, *Solitons and the inverse scattering transforms*. SIAM, Philadelphia, 1981.